Chapter 18
Green Preparation and Environmental Applications of Some Electrospun Fibers

Juanjuan Yin, Qingrui Zhang, Lexin Zhang, Jingxin Zhou, and Tifeng Jiao

1 Introduction

Electrospinning technology is a technology for preparing polymer micro–nano-fibers [1–3]. This technology is simple and easy to operate and has high production efficiency. A thin-film composite of continuous nanoscale fibers can be prepared from a polymer solution. The electrostatic spinning device is mainly composed of three parts: high voltage power supply, spinning head, and receiving screen. Under the action of electric field force, the charges on the surface of the droplet at the tip of the spinning needle are concentrated and repel each other, and the droplet is elongated to form a Taylor cone [4, 5]. After spraying out, it solidifies in the air and finally forms disorderly arranged nanofibers on the receiving device. Under the impetus of the stepping pump, the spinning continued, and the fine stream ejected from the needle was continuously deposited on the receiving screen and finally formed a film product woven by nanofibers [6, 7]. In recent decades, the research on electrospinning has mainly focused on the development of electrospinning nanofiber raw materials, multi-component polymer electrospinning, and electrospinning jet instability models.

Electrospinning technology has many outstanding advantages, such as no complicated and expensive equipment and instruments, and lower experimental costs. In addition, the operation of electrospinning is simple and easy, and the applicable raw materials are widely free from harsh requirements. The most important thing is that the prepared fibers are at the nanometer level, and the average fiber diameter is generally between tens and hundreds of nanometers. Therefore, the resulting film has the characteristics of controllable fiber diameter [8], high tensile strength [9,

J. Yin · Q. Zhang · L. Zhang · J. Zhou · T. Jiao (✉)
Hebei Key Laboratory of Applied Chemistry, School of Environmental and Chemical Engineering, Yanshan University, Qinhuangdao 066004, China
e-mail: tfjiao@ysu.edu.cn

S. Thomas and P. Balakrishnan (eds.), *Green Composites*, Materials Horizons: From Nature to Nanomaterials,
https://doi.org/10.1007/978-981-15-9643-8_18

10], and very large surface area [11–17]. Therefore, these advantages make the electrospun nanofiber film have a wide range of potential applications in many fields, including tissue engineering [18], drug sustained-release [19], nanosensors [20], energy applications [21], biochips and catalyst loading.

At present, the construction of nanostructures of various materials (such as polymers, inorganics, and multi-component composites) has been achieved through electrospinning technology [22–24], which has shown great abilities in the fields of catalysis, drug carriers, and filtration potential [25, 26]. Liu et al. have successfully prepared a new composite film based on silver nano-particles modified polyvinyl alcohol/polyacrylic acid/carboxyl functionalized graphene oxide (PVA/PAA/GO-COOH@AgNPs) as Efficient Dye Photocatalyst Materials for Wastewater Treatment [27]. Panaitescu et al. processed modified poly(3-hydroxybutyrate) by using nanocellulose and plasma technology as a candidate material for food packaging applications [28]. Rauwel et al. introduced several nanomaterials in the book "Application and Behavior of Nanomaterials in Water Treatment", such as graphene/CNT and nanostructured Prussian blue hybrid nanocomposites, controlled growth of LDH films and rod-shaped MnO nanocomposites, and so on. It is applied to sewage treatment, and a good purification effect is obtained [29]. In addition, the fiber material shows good adsorption capacity due to its microporous structure. This chapter provides a comprehensive review of the preparation process of various electrospun fiber materials and applies these composite nanofiber materials to the fields of adsorption, catalysis, and air filtration. It also provides challenges and prospects to inspire more exciting developments in the future.

2 Preparation of Electrospinning Nanocomposite Membrane and Its Adsorption and Degradation of Organic Dyes in Wastewater

The preparation of electrospun nanocomposite membranes has been a hot topic in many fields, such as chemistry, materials science, and nanotechnology. In this section, we will focus on the application of different types of polymer nanofilms in the adsorption and degradation of organic dyes: (i) bioinspired polydopamine sheathed nanofibers containing carboxylate graphene oxide nanosheet for high-efficient dyes scavenger, (ii) preparation of TiO_2 nanoparticles modified electrospun nanocomposite membranes toward efficient dye degradation for wastewater treatment, (iii) polydopamine-coated electrospun poly(vinyl alcohol)/poly(acrylic acid) membranes as efficient dye adsorbent with good recyclability, (iv) fabrication and highly efficient dye removal characterization of beta-cyclodextrin-based composite polymer fibers by electrospinning, and (v) self-assembled AgNP-containing nanocomposites constructed by electrospinning as efficient dye photocatalyst materials for wastewater treatment.

2.1 Bioinspired Polydopamine Sheathed Nanofibers Containing Carboxylate Graphene Oxide Nanosheet for High-Efficient Dyes Scavenger

Firstly, Xing et al. successfully prepared a new type of hierarchical bioinspired nanocomposite materials of poly(vinyl alcohol)/poly(acrylic acid)/carboxylate graphene oxide nanosheet@polydopamine (PVA/PAA/GO-COOH@PDA) by electrospinning technique, thermal treatment, and polydopamine modification [30]. The obtained composite membranes are composed of polymeric nanofibers with carboxylate graphene oxide nanosheets, which are anchored on the fibers by the heat-induced crosslinking reaction. The preparation process demonstrates an eco-friendly and controllable manner. These as-formed nanocomposites were characterized by various morphological methods and spectral techniques. Due to the unique polydopamine and graphene oxide containing structures in composites, the as-obtained composite demonstrates well-efficient adsorption capacity toward dye removal, which is primarily due to the specific surface area of electrospun membranes and the active polydopamine/graphene oxide components [31–33]. In addition, it should be noted that the adsorption capacities of the as-obtained PVA/PAA/GO-COOH@PDA nanocomposites on MB show better performance than two other used dyes. The main reason for the difference can be speculated to the matched strong π–π stacking and electrostatic interactions between nanocomposites and MB molecules. At the same time, the abundant amino and hydroxyl groups in the PDA surface give more adsorbent activity points for dye molecules, which demonstrate the tailored strategy to improve the absorption performance (Figs. 1 and 2).

Therefore, the present work is expected to open a new avenue for the design and preparation of eco-friendly electrospun composites loaded with functional GO and nanoparticles, which could enhance the practical application in wastewater treatment by using functionalized composite nanofibers materials.

2.2 Preparation of TiO_2 Nanoparticles Modified Electrospun Nanocomposite Membranes Toward Efficient Dye Degradation for Wastewater Treatment

Firstly, Hou et al. prepared nano-polyvinyl alcohol/polyacrylic acid/carboxyl functionalized graphene oxide nanocomposite films by using electrospinning technology [34]. The composite membrane prepared by electrospinning technology is composed of polymer nanofibers with carboxyl functionalized graphene oxide sheets, which are anchored to the fibers through a thermally induced crosslinking reaction. TiO_2 nanoparticles are deposited uniformly and uniformly on the surface of the resulting composite film. The preparation process of the nano-composite membrane is simple, green, and environmentally friendly, and it is easy to operate and control. The prepared composite membranes exhibited an effective photocatalytic ability for dye

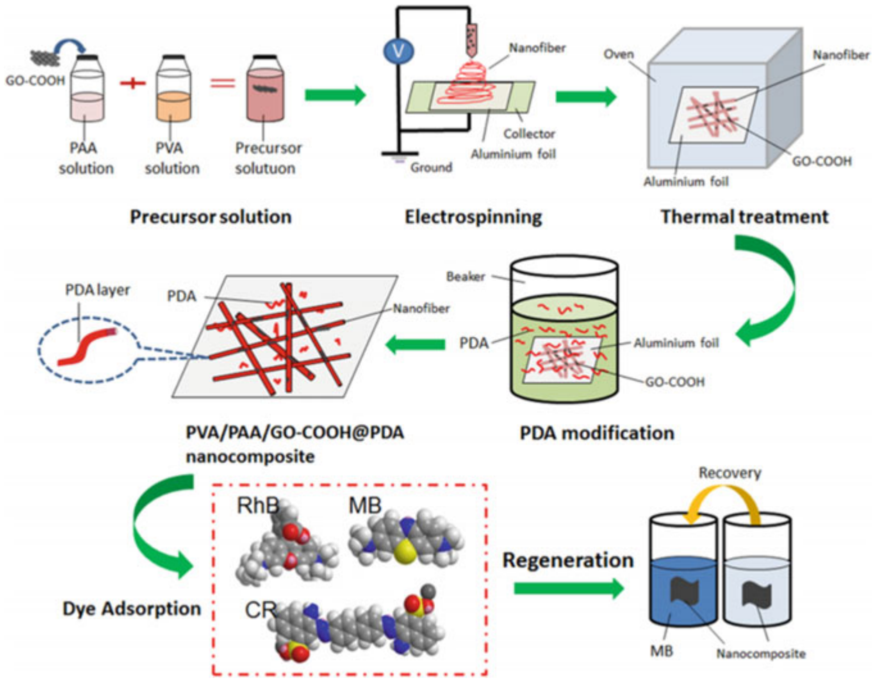

Fig. 1 Schematic illustration of the fabrication and dye adsorption of PVA/PAA/GO-COOH@PDA nanocomposites by electrospinning and thermal treatment. Reproduced with permission from Ref. [30]. Copyright 2017, American Chemical Society

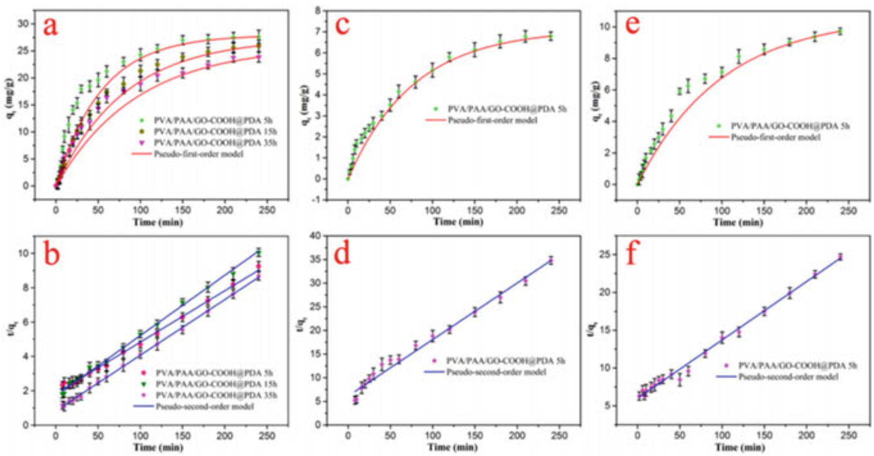

Fig. 2 Adsorption kinetics curves of as-prepared PVA/PAA/GO-COOH@PDA nanocomposites on MB (**a**, **b**), RhB (**c**, **d**), and CR (**e**, **f**) at 298 K. Reproduced with permission from Ref. [30]. Copyright 2017, American Chemical Society

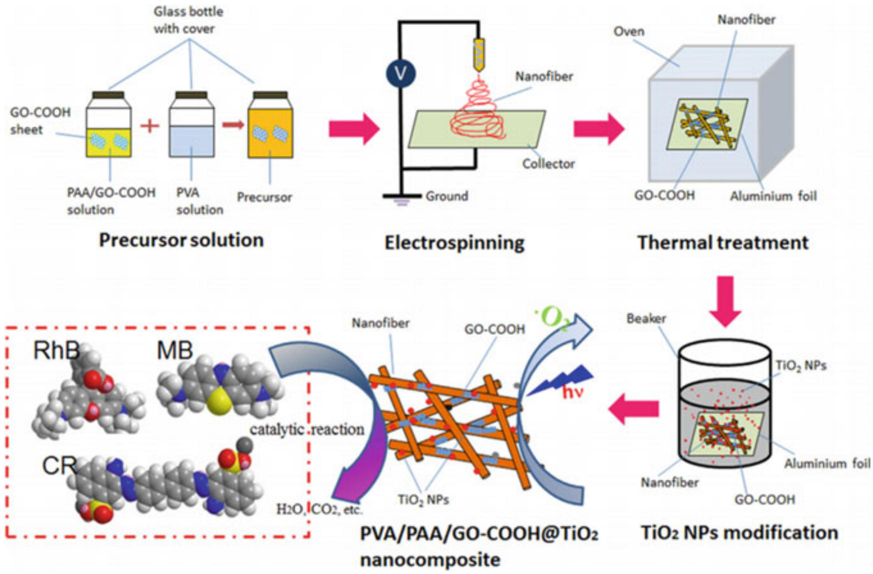

Fig. 3 Schematic illustration of the fabrication of PVA/PAA/GO-COOH@TiO_2 nanocomposite by electrospinning and thermal treatment. Reprinted with permission from Ref. [34]. Copyright 2017, Elsevier Ltd

degradation, which was mainly attributed to the specific surface area of electrospun membranes and the photoactivity of TiO_2 nanoparticles. In addition, the composite membrane reported here is easy to regenerate, which indicates potential large-scale applications in wastewater treatment and dye removal (Figs. 3, 4 and Table 1).

At the same time, the author also studied the photocatalytic performance of the prepared PVA/PAA/GO-COOH@TiO_2 nanocomposite membrane to three model dye solutions (CR, RhB, and MB). The degradation program currently studied was characterized by placing the obtained PVA/PAA/GO-COOH@TiO_2 nanocomposites in different aqueous dye solutions [35–40]. In addition, this catalytic experiment was measured and repeated three times. The degradation kinetics experiments of the prepared PVA/PAA/GO-COOH@TiO_2 nanocomposites were carried out. The results are shown in Fig. 4. This work is expected to open up a new way for the design and preparation of environmentally friendly electrospun composite materials containing functional GO and nanoparticles. The use of functional composite nanofiber materials can enhance the practical application of wastewater treatment.

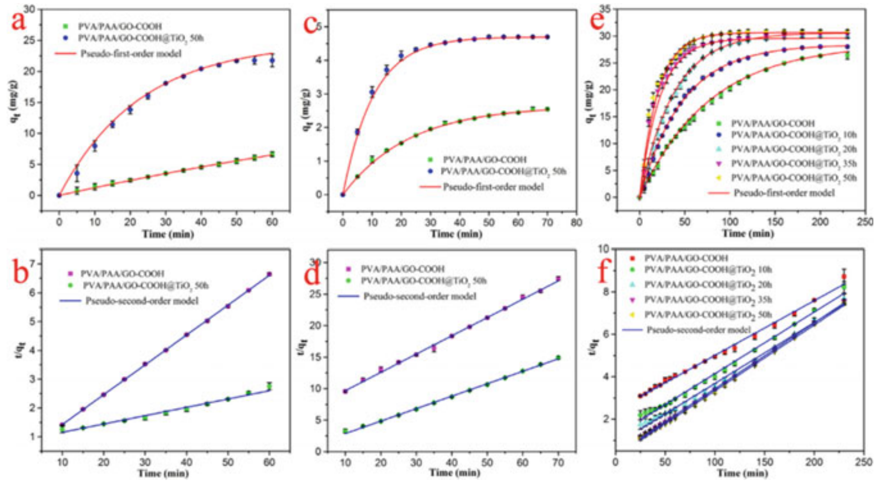

Fig. 4 Photocatalytic kinetics curves of as-prepared PVA/PAA/GO-COOH@TiO_2 nanocomposite on CR (**a** and **b**), RhB (**c** and **d**), and MB (**e** and **f**) at 298 K. Reprinted with permission from Ref. [34]. Copyright 2017, Elsevier Ltd

2.3 Polydopamine-Coated Electrospun Poly(Vinyl Alcohol)/poly(Acrylic Acid) Membranes as Efficient Dye Adsorbent with Good Recyclability

Inspired by the characteristics of adhesion proteins in marine mussels, dopamine, which is a catecholamine, can self-polymerize under alkaline reaction conditions and form a polydopamine (PDA) film on almost all types of substrates [41, 42]. The PDA coating can form a highly stable polymer layer on the target surface and shows special adhesion in the presence of residual catechol groups on the PDA layer, which helps to further react with appropriate molecules; it also provides the possibility for customized PDA coatings for various applications [43]. For example, PDA membranes are often used as modifiers to improve the hydrophilicity and reactivity of target substrates (such as clay [44], polystyrene nanofibers [45], and even polytetrafluoroethylene [46]). In particular, Gao et al. prepared a PDA-functionalized graphene hydrogel in a one-step process and found that the PDA-coated graphene hydrogel has good adsorption capacity for heavy metals and organic dyes in wastewater [47]. Recently, nanoparticles decorated with PDA (such as Fe_3O_4 [48] and natural zeolite [49]) have also been synthesized and used to remove various pollutants. However, considering the above-environmental issues, we should focus on the use of polydopamine as an adsorbent to remove dye contaminants in water for more research.

Table 1 Kinetic parameters of PVA/PAA/GO-COOH nanocomposite and PVA/PAA/GO-COOH@TiO_2 nanocomposite for CR, RhB, and MB (e and f) degradations and removal at 298 K (experimental data from Fig. 4)

CR	Pseudo-first-order model			Pseudo-second-order model		
	q_e (mg/g)	R^2	k_1 (min^{-1})	q_e (mg/g)	R^2	k_2 (g/mg min)
PVA/PAA/GO-GOOH	8.661	0.964	0.1204	9.662	0.9998	0.0272
PVA/PAA/G0-C00H@$Ti0_2$ 50 h	24.52	0.9955	0.0447	33.57	0.9779	0.0011
RhB	Pseudo-first-order model			Pseudo-second-order model		
	q_e (mg/g)	R^2	k_1 (min^{-1})	q_e (mg/g)	R^2	k_2 (g/mg min)
PVA/PAA/GO-GOOH	2.642	0.9981	0.0442	3.431	0.9976	0.0125
PVA/PAA/G0-C00H@$Ti0_2$ 50 h	4.691	0.9997	0.096	5.112	0.9983	0.0387
MB	Pseudo-first-order model			Pseudo-second-order model		
	q_e (mg/g)	R^2	k_1 (min^{-1})	q_e (mg/g)	R^2	k_2 (g/mg min)
PVA/PAA/GO-GOOH	28.56	0.9989	0.0129	38.79	0.9939	2.73×10^{-4}
PVA/PAA/G0-C00H@$Ti0_2$ 10 h	28.42	0.998	0.02096	4.29	0.9949	6.86×10^{-4}
PVA/PAA/G0-C00H@$Ti0_2$ 20 h	30.56	0.9971	0.02671	34.77	0.994	1.03×10^{-3}
PVA/PAA/G0-C00H@$Ti0_2$ 35 h	29.66	0.9879	0.04191	32.16	0.9995	2.89×10^{-3}
PVA/PAA/G0-C00H@$Ti0_2$ 50 h	30.45	0.9903	0.05228	32.22	0.9989	3.10×10^{-3}

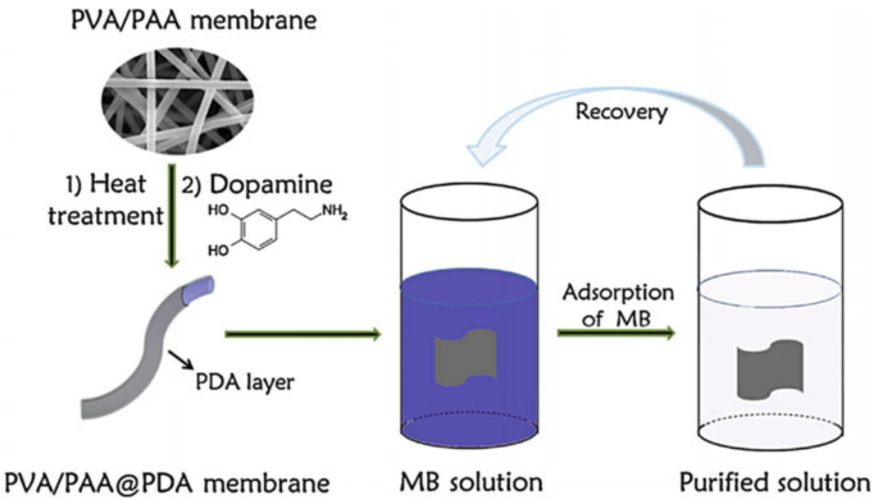

Fig. 5 Schematic illustration of the preparation of PVA/PAA@PDA membranes and their applications for dye adsorption. Reprinted with permission from Ref. [50]. Copyright 2015, Elsevier Ltd

Yan et al. prepared a free-standing polyvinyl alcohol/polyacrylic acid (PVA/PAA) film with polydopamine (PDA) coating based on electrospinning and self-polymerization of dopamine [50]. The preparation process is simple, green, controllable, and low energy consumption, and there are no strict restrictions on the reaction conditions. Thanks to the high specific surface area of electrospun membranes and the rich "adhesive" functional groups of polydopamine, the membranes produced exhibited effective adsorption properties for methyl blue, with an adsorption capacity of up to 1147.6 mg g^{-1}. Moreover, compared with other nanoparticle adsorbents, the prepared free-standing membrane has high flexibility and is easy to handle and recycle, and the most important thing is easy to elute and regenerate so that it has potential applications in wastewater treatment prospect (Figs. 5 and 6).

2.4 Fabrication and Highly Efficient Dye Removal Characterization of Beta-Cyclodextrin-Based Composite Polymer Fibers by Electrospinning

As a class of cyclic oligosaccharides, cyclodextrins have hollow cones, which have external hydrophilicity and internal hydrophobicity. This special structure has many special physical and chemical properties. It can selectively bind small organic molecules in aqueous solution, and the formed inclusion complex has different degrees of stability [51–53]. Therefore, cyclodextrins and its derivatives are widely

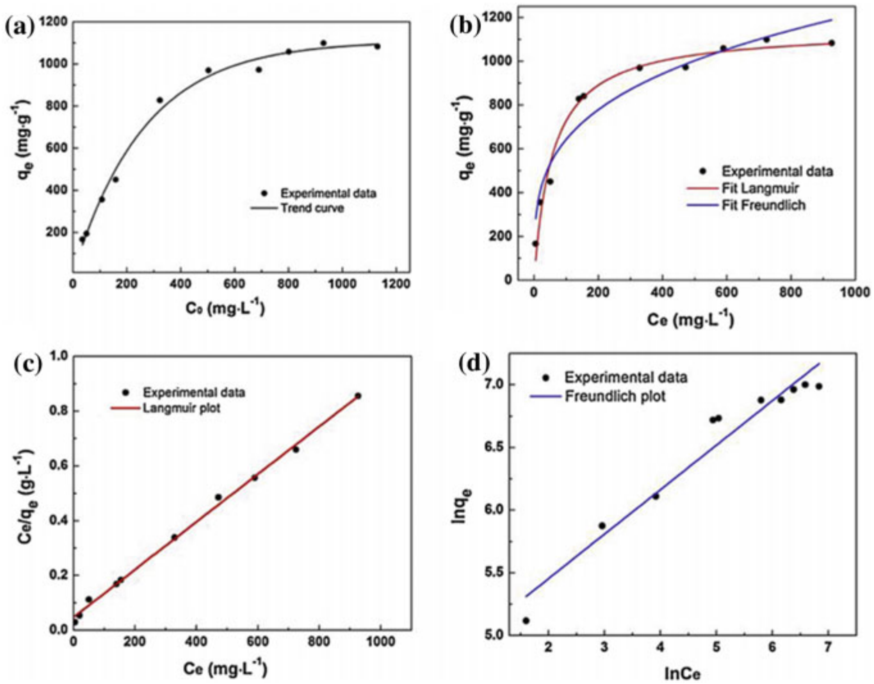

Fig. 6 Adsorption isotherms (**a** and **b**) and the corresponding Langmuir plot (**c**), Freundlich plot (**d**) for MB adsorption on PVA/PAA@PDA-15 membrane. Reprinted with permission from Ref. [50]. Copyright 2015, Elsevier Ltd

used in medicine, food, chemical engineering materials, especially wastewater treatment [54–58]. For example, Li et al. prepared a material based on cyclodextrins to remove malachite green [59]. The adsorption results are in accordance with the Langmuir model, and the maximum adsorption capacity reaches 91.9 mg/g. Yilmaz et al. synthesized two polymers based on β-cyclodextrin with the aid of 4, 4′-methylene-bis-phenyldiisocyanate (MDI) or hexamethylene diisocyanate (HMDI) [60]. These materials can remove azo dyes and aromatic amines, and the main adsorption mechanism is the host–guest interaction. At present, some cyclodextrin-based fiber systems by electrospinning have been reported. For example, Cui et al. described the use of plasma-treated polyethylene oxide-β-cyclodextrin nanofibers to enhance antibacterial activity [61]. Celebioglu et al. demonstrated electrospinning of polymer-free nanofiber structures formed from inclusion compounds between hydroxypropyl-β-cyclodextrin and vitamin E [62]. The prepared vitamin E-containing fiber web provides enhanced photostability of sensitive vitamin E by inclusion complexes even after exposure to UV light.

Guo et al. prepared a new type of composite fiber adsorption material composed of ε-polycaprolactone (PCL) and β-cyclodextrin-based polymer (PCD) by electrospinning, used to solve the increasing pollution of azo dye problem [63]. More importantly, PCD was chosen because of its infinite long chain and cavity structure. Due to a large number of free cyclodextrin pores on the fiber surface, the resulting membrane helps to form more host–guest interactions. Therefore, according to previous reports [64], its excellent selective adsorption capacity can be foreseen. During the electrospinning process, long-chain polymer molecules may occupy some cyclodextrin cavities, which is not conducive to the interaction between the host and the guest and even leads to the reduction of poor adsorption. However, our PCL/(n%) PCD composite fiber has countless holes, which can guarantee selective adsorption capacity. Therefore, it is obvious that the PCL/(n%) PCD composite fibers obtained can exhibit significant adsorption capacity for azo dyes and have host–guest interactions. Moreover, the introduction of a β-cyclodextrin polymer can effectively improve the mechanical strength and stability of the membrane. This shows that the obtained composite material has great potential, which can help the problem of azo dye pollution in wastewater treatment (Figs. 7, 8 and 9).

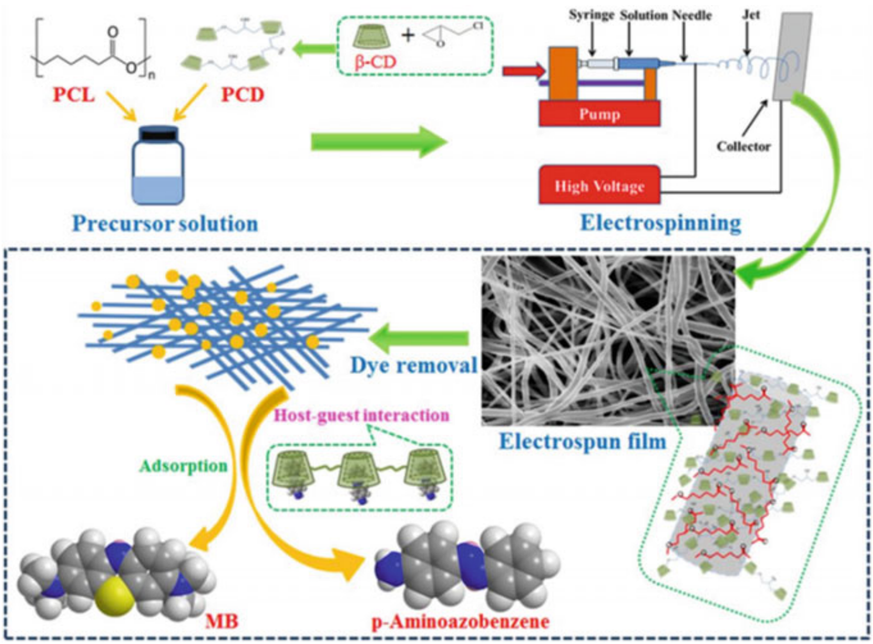

Fig. 7 Schematic illustration of preparation and application in dye removal of PCL/(n%)PCD composite fibers by electrospinning. Reprinted with permission from Ref. [63]. Copyright 2019, MDPI Ltd

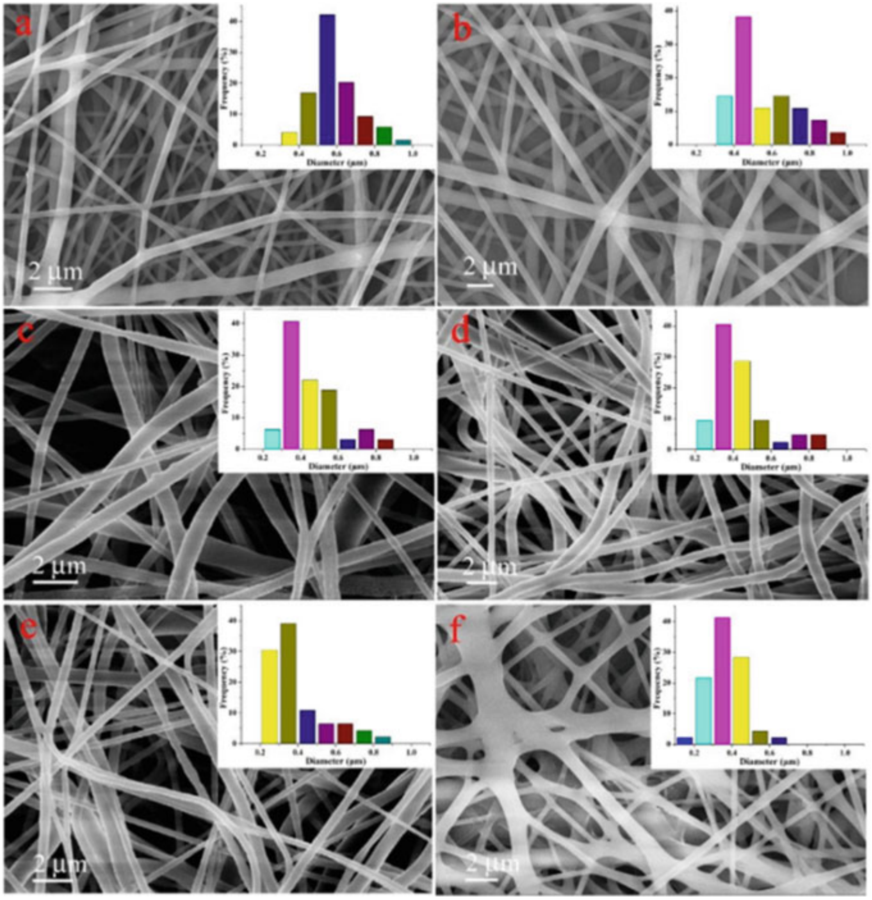

Fig. 8 SEM images and diameter distribution histograms of neat PCL fibers (**a**), PCL/(10%)PCD(**b**), PCL/(20%)PCD(**c**), PCL/(30%)PCD (**d**), PCL/(40%)PCD (**e**), and PCL/(50%)PCD (**f**). Reprinted with permission from Ref. [63]. Copyright 2019, MDPI Ltd

2.5 Self-assembled AgNP-Containing Nanocomposites Constructed by Electrospinning as Efficient Dye Photocatalyst Materials for Wastewater Treatment

Graphene oxide (GO)-based nanocomposite fibers have attracted great interest due to their adjustable dispersibility, large oxygen-containing functional groups, and special chemical modification and preferred reaction positions/sites [65]. Liu et al. have successfully prepared a new composite film based on silver nanoparticles modified polyvinyl alcohol/polyacrylic acid/carboxyl functionalized graphene oxide (PVA/PAA/GO-COOH@AgNPs) [27]. The new composite membrane utilizes the advantages of graphene oxide (GO) nanocomposites and many novel advantages of

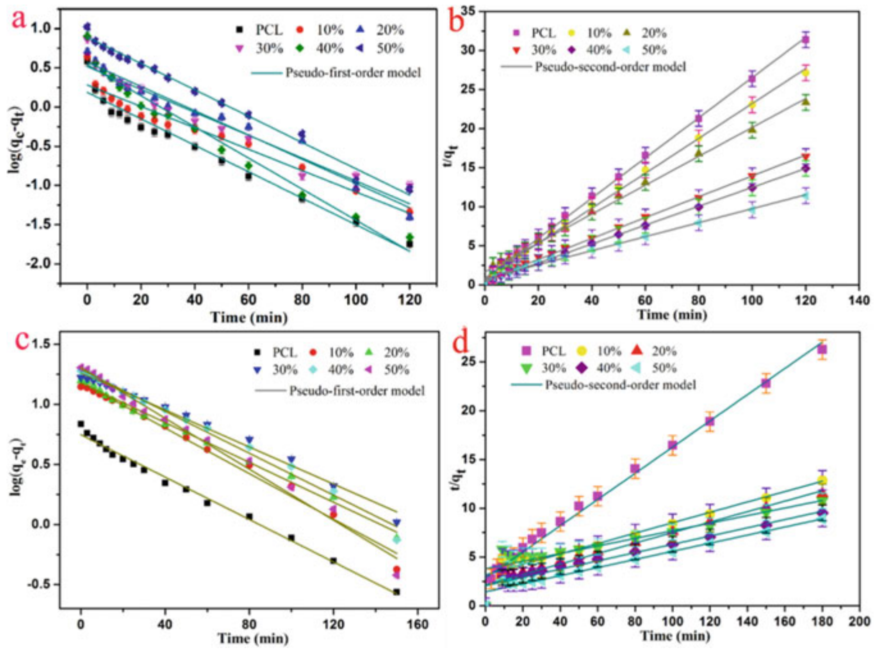

Fig. 9 Kinetic adsorption of MB (**a**,**b**) and 4-aminoazobenzene (**c**, **d**). Reprinted with permission from Ref. [63]. Copyright 2019, MDPI Ltd

electrospun fibers. At the same time, the Ag nanoparticles produced by the reduction of ascorbic acid solution to $AgNO_3$ are firmly fixed in the nanometer using hydrogen bonding and electrostatic interaction with the surface of the fiber. First, due to its chemical and mechanical properties and large specific surface area, the prepared PVA/PAA/GO-COOH system was selected as the matrix material for electrospinning [66]. Secondly, compared with conventional organic solvents, deionized water is used as a solvent for preparing electrospinning solutions, which has the characteristics of low cost and environmental friendliness. Most importantly, Ag nanoparticles show that they can achieve good stability between the flexible surface of the fiber and the effective GO nanosheets and function under visible light. The powerful π–π force in the GO sheet can make various dyes in water have strong adsorption force. In addition, the fixed carboxyl groups in GO nanosheets can generate strong electrostatic interactions through their highly negatively charged characteristics, which can promote the diffusion and enrichment of target dyes. For the degradation of MB, the prepared PVA/PAA/GO-COOH@AgNPs nanocomposite membranes still have significant catalytic activity even after eight catalytic degradations at room temperature. Therefore, the author provides a green and novel method to prepare highly efficient dye photocatalytic wastewater treatment materials (Fig. 10).

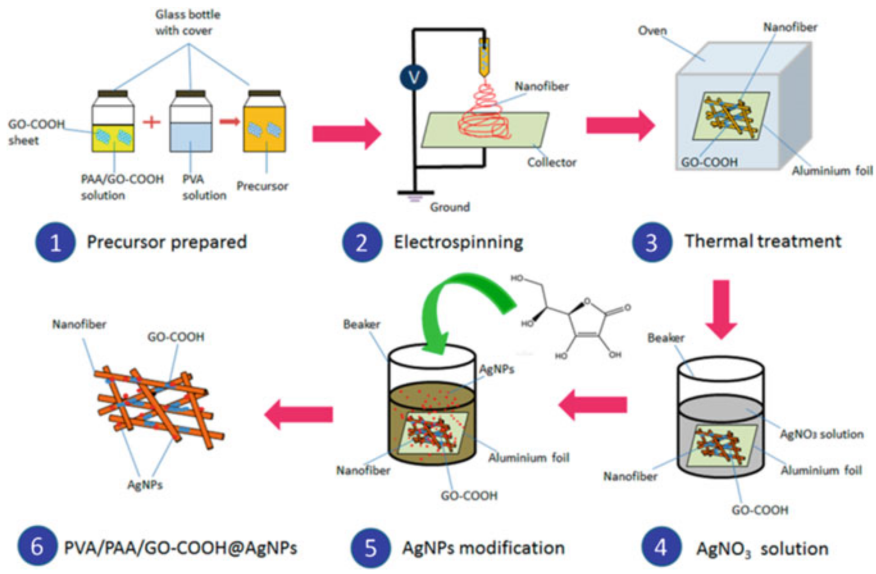

Fig. 10 Schematic illustration of the fabrication of PVA/PAA/GO-COOH@AgNPs nanocomposites by electrospinning and thermal treatment. Reprinted with permission from Ref. [27]. Copyright 2018, MDPI Ltd

3 Preparation of Electrospun Nanofiber and Characterization of Catalytic Performance

3.1 Scalable Fabrication of Nanoporous Carbon Fiber Films as Bifunctional Catalytic Electrodes for Flexible Zn-Air Batteries

With the rapid development of flexible and wearable optoelectronic devices, there is an urgent need to use flexible high-density energy storage devices as the power source [67]. Recently, people have made tremendous efforts to develop flexible lithium-ion batteries and supercapacitors. However, due to the low energy density of the batteries and the limited cycle life, it has become a research difficulty [68]. Because metal–air batteries are said to have high energy capacity [69], they are the next generation of promising wearable optoelectronic products for energy storage devices. Of particular concern is that zinc–air batteries have received extensive research and development attention due to their high energy density, low cost, and high safety [70]. However, most cathodes currently used in zinc–air batteries are bulky and rare. Meet the specific requirements of flexible Zn-air batteries. In addition, the development of highly efficient dual-functional electrocatalysts for the oxygen reduction reaction (ORR) and oxygen release reaction (OER) of flexible rechargeable zinc–air batteries remains a huge challenge [71], although important progress has been made recently used in traditional zinc–air batteries [72] (Figs. 11, 12 and 13).

Liu et al. found that newly developed nanoporous carbon nanofiber films (NCNFs) with the large specific surface areas are flexible and show that they are excellent when used as air cathodes in liquid Zn-air batteries used in ambient air [73]. The performance has a high open-circuit voltage (1.48 V), maximum power density (185 mW cm^{-2}), and energy density (776 Wh kg-1) and has a large specific surface area (1249 m^2 g^{-1}), high electrical conductivity (147 S m^{-1}), moderate tensile strength (1.89 MPa), and tensile modulus (0.31 GPa). They show excellent performance for ORR (initial potential = 0.97 V vs RHE; limiting current density = 4.7 mA cm^{-2}) and OER (initial potential = 1.43 V vs RHE, potential = 1.84 V @ 10 mA cm^{-2}) dual-function electrocatalytic activity.

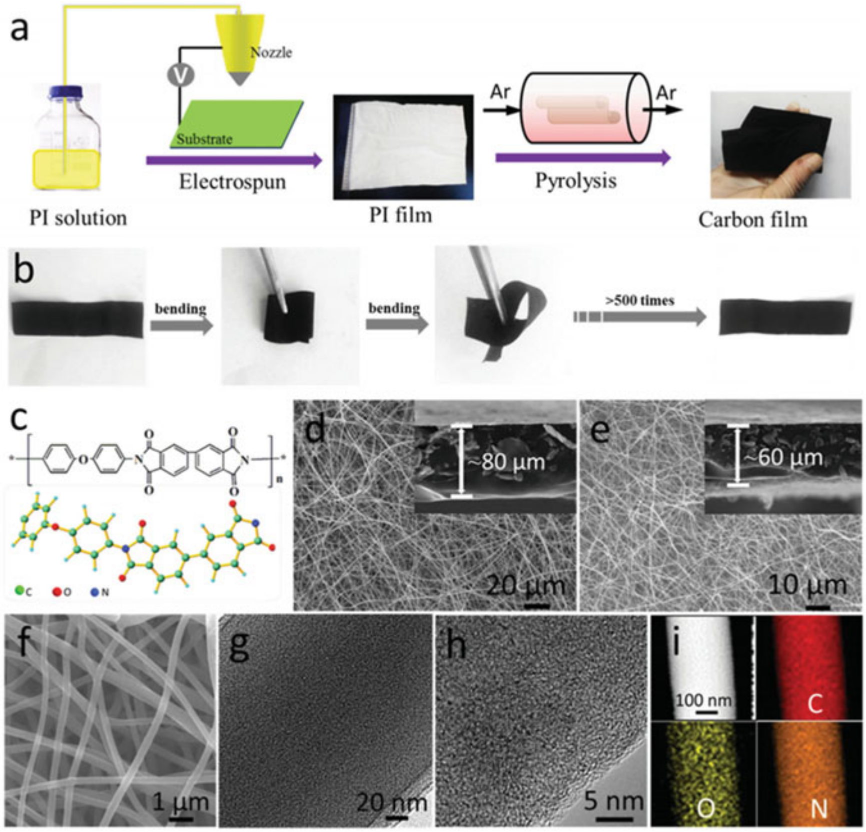

Fig. 11 **a** Schematic representation of the fabrication procedure toward the NCNF. **b** Photographs of the resultant flexible NCNF. **c** Chemical structure of PI polymer. SEM images of **d** the pristine PI film and **e**, **f** NCNF-1000. **g**, **h** HRTEM, **i** STEM images and corresponding elemental mapping images of C, O, N of NCNF-1000. Reprinted with permission from Ref. [73]. Copyright 2016, Wiley-Blackwell

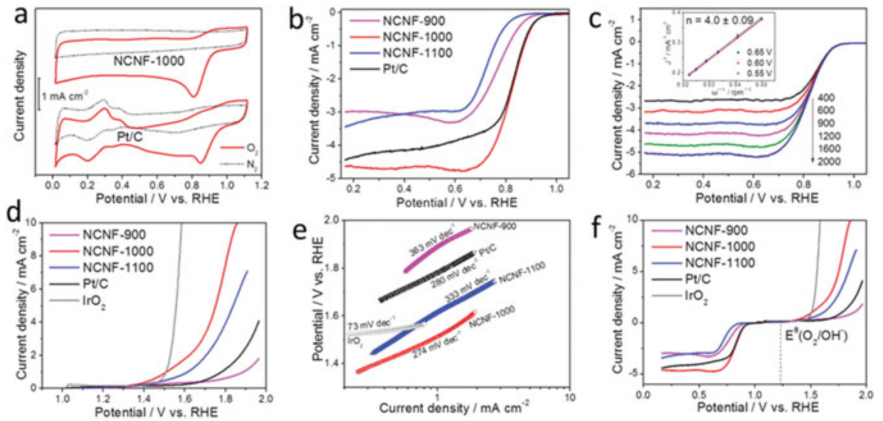

Fig. 12 **a** CV curves of NCNF-1000 and Pt/C, in O_2-saturated (solid line) and N_2-saturated (dotted line) 0.1 M KOH. **b** LSV curves of different catalysts for ORR in O_2-saturated at 1600 rpm. **c** LSV curves of NCNF-1000 for ORR at different rotating speeds and the inset is K-L plots of NCNF-1000 at different potentials including the calculated number of electron transfer (n) per O_2. **d** LSV curves of different catalysts for OER at 1600 rpm in 0.1 M KOH. **e** Tafel slopes derived from (**d**). **f** LSV curves of different catalysts for both ORR and OER in 0.1 M KOH at 1600 rpm (scan rate 5 mV s^{-1}). The catalyst loading was 0.1 mg cm^{-2} for all catalysts. Reprinted with permission from Ref. [73]. Copyright 2016, Wiley-Blackwell

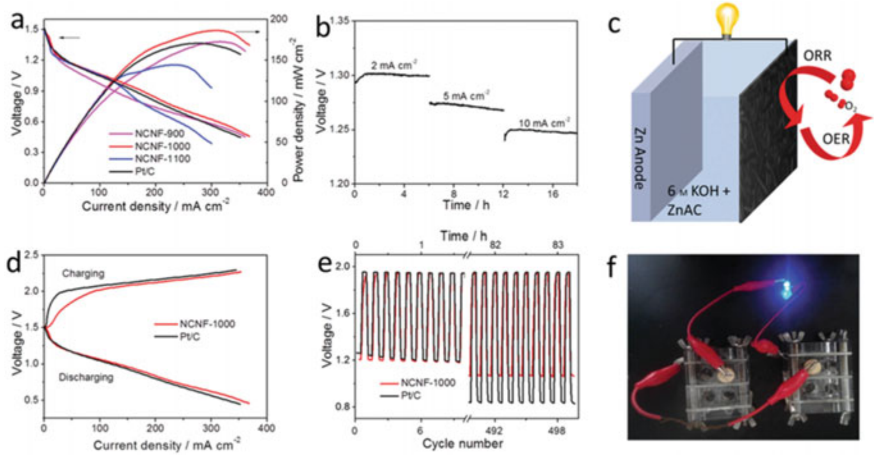

Fig. 13 **a** Polarization and power density curves of the primary Zn-air batteries with different catalysts. **b** Galvanostatic discharge curves of the primary Zn-air battery with NCNF-1000 as a catalyst at different current densities, which was normalized to the area of air–cathode. **c** Schematic representation of the rechargeable Zn-air battery. **d** Charge and discharge polarization curves. **e** Galvanostatic discharge–charge cycling curves at 10 mA cm^{-2} of rechargeable Zn-air batteries with the NCNF-1000 and Pt/C as catalyst, respectively. **f** Photograph of a blue LED (≈3.0 V) powered by two liquid Zn-air batteries with the NCNF-1000 air–cathode connected in series. Reprinted with permission from Ref. [73]. Copyright 2016, Wiley-Blackwell

3.2 Carbon Nanofiber-Supported PdNi Alloy Nanoparticles as Highly Efficient Bifunctional Catalysts for Hydrogen and Oxygen Evolution Reactions

Currently, much attention is focused on developing efficient and clean renewable energy technologies to increase energy demand and alleviate environmental problems [74–76]. As we all know, the production of hydrogen through water electrolysis is a key strategy to overcome these energy challenges [77–79]. However, the water decomposition half-reactions, namely the hydrogen evolution reaction (HER) and the oxygen evolution reaction (OER), have a high overpotential and are high energy [80, 81]. An effective electrocatalyst is essential to enhance the electrochemical water-splitting performance. In particular, precious metal catalysts (such as Pt and RuO_2) have been used as the most advanced electrocatalysts for HER and OER, respectively [82–84]. However, the high cost and low global reserves of these metals limit their wide practical application. In addition, a catalyst capable of driving both HER and OER is very needed, which is a basic requirement as a high-efficiency energy conversion device in water decomposition. Unfortunately, it is relatively difficult to develop effective, durable, and cost-effective bifunctional catalysts for HER and OER. Note that highly efficient bifunctional catalysts with high HER and OER activity are still highly desired. Chem et al. prepared carbon nanofiber-loaded PdNi alloy nanoparticles, a highly efficient dual-function catalyst for hydrogen and oxygen release reactions [85].

A new class of the PdNi alloy structure was prepared on CNFs by electrospinning and subsequent carbonization. The as-synthesized PdNi/CNFs, which have a low Pd loading, exhibit superior catalytic activity, and good stability in both the HER and OER and are thus a promising alternative bifunctional electrocatalyst. The highly efficient catalytic performance of the PdNi/CNFs is attributed to the synergistic effects of the PdNi alloy and the properties of the CNF substrate. The combination of these factors enhances the catalytic activity and is expected to enable the realization of cost-effective hydrogen and oxygen generation. Therefore, the catalyst developed in this work could be suitable for use in various water-splitting applications (Figs. 14, 15 and 16).

3.3 Preparation of Palladium Nanoparticles Decorated Polyethyleneimine/Polycaprolactone Composite Fibers Constructed by Electrospinning with Highly Efficient and Recyclable Catalytic Performances

In recent years, in the context of rapid technological and economic development, available water sources are increasingly scarce, and people have paid extensive attention to the protection and purification of water. Hazardous organic waste is the main

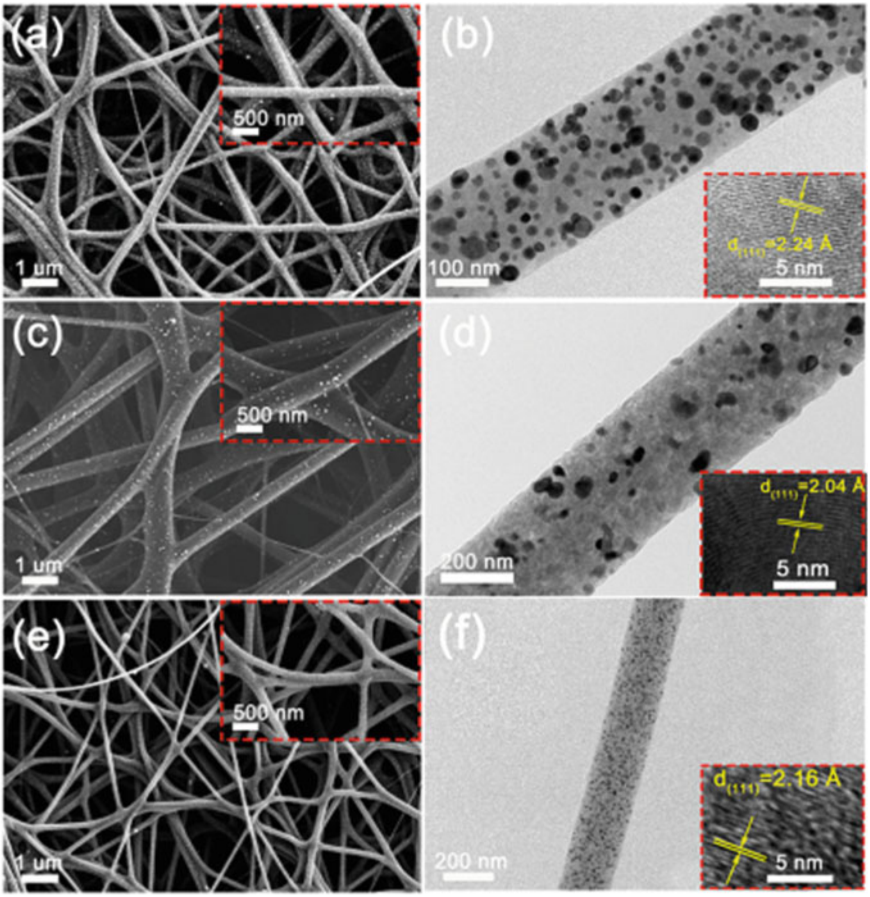

Fig. 14 **a**, **c**, **e** FE-SEM and **b**, **d**, **f** TEM images of the Pd/CNFs (**a**, **b**), Ni/CNFs (**c**, **d**) and PdNi/CNFs-1:2 (**e**, **f**). The insets are the corresponding HRTEM images. Reprinted with permission from Ref. [85]. Copyright 2017, Elsevier Ltd

source of water pollution [86–92]. The conversion of harmful organic chemicals into harmless or low-toxic compounds under mild conditions has become an extremely important research field [93–95]. As we all know, 4-nitrophenol (4-NP) is widely used in the synthesis of dyes and drugs and is one of the chemical products commonly used in the chemical industry [96].

Nano-sized palladium nanoparticles show high catalytic activity due to the tendency of aggregation and have serious limitations in the field of catalysis. A solid substrate with a large specific surface area is an ideal carrier for palladium nanoparticles. Wang et al. successfully designed and prepared polyethyleneimine/polycaprolactone/Pd nanoparticles (PEI/PCL@PdNPs) composite catalyst by electrospinning and reduction method using PEI/PCL electrospun fiber as the carrier [97]. A large number of pit structures increase the specific

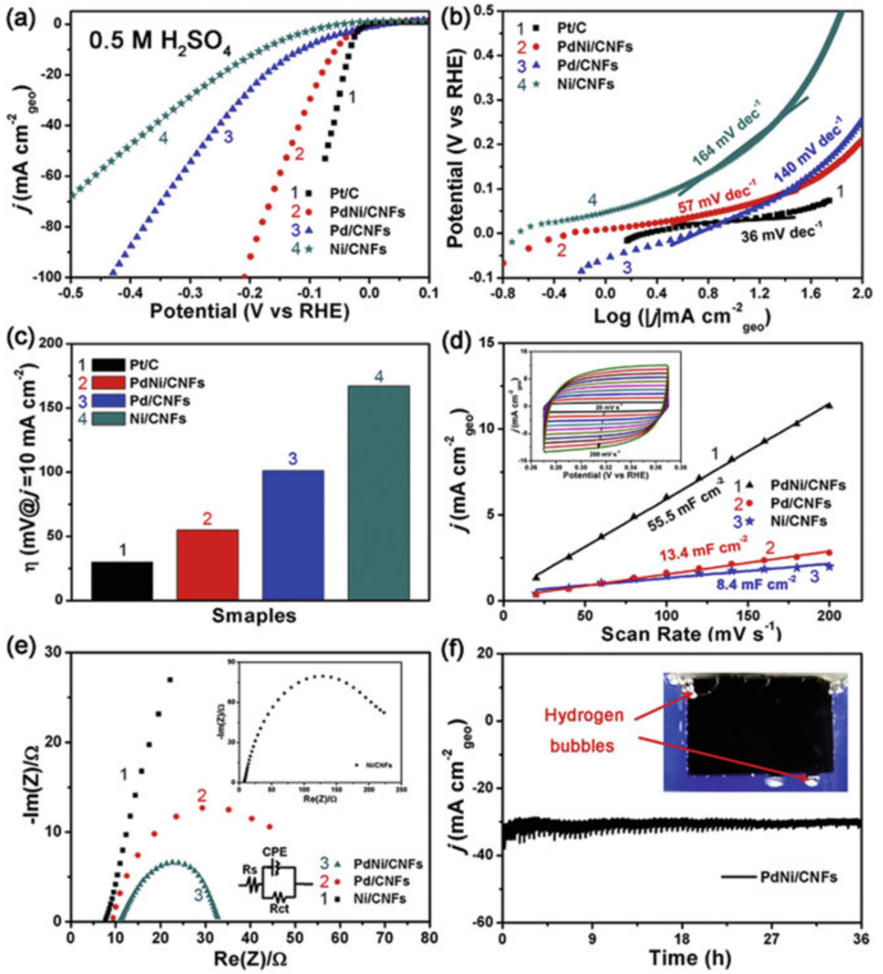

Fig. 15 HER electrocatalysis in 0.5 M H_2SO_4. **a** Polarization curves and **b** corresponding Tafel plots of the Pd/CNFs, Ni/CNFs, PdNi/CNFs-1:2 and commercial Pt/C catalyst; **c** Histograms of overpotentials at $j = 10$ mA cm^{-2} for the catalysts of Pd/CNFs, Ni/CNFs, PdNi/CNFs-1:2 and commercial Pt/C; **d** The linear fit of the capacitive currents of the catalysts versus the scan rates, inset in (**d**) is the electrochemical cyclic voltammograms of Pd/CNFs at potential scanning rates from 20 mV s^{-1} to 200 mV s^{-1}; **e** EIS of the Pd/CNFs, Ni/CNFs and PdNi/CNFs-1:2 at the potential of 0.1 V versus RHE (the insets show the equivalent circuit of the fitted curves and the full EIS spectrum of the Ni/CNFs); **f** chronoamperometric response (j-t) curve of PdNi/CNFs-1:2 at a constant voltage of 50 mV versus RHE (the insets show a digital image of the H2 bubbles formed on the PdNi/CNFs-1:2 membrane during the electrocatalytic process). Reprinted with permission from Ref. [85]. Copyright 2017, Elsevier Ltd

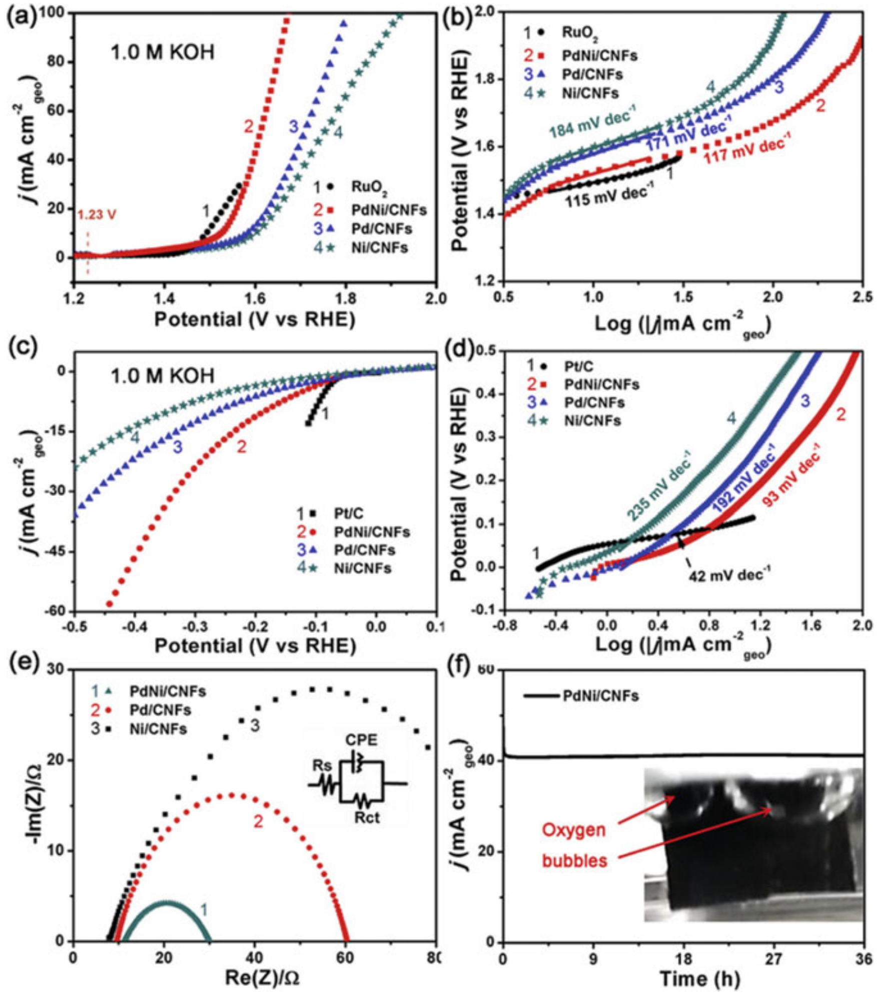

Fig. 16 OER and HER electrocatalysis in 1 M KOH. **a** Polarization curves and **b** corresponding Tafel plots of the Pd/CNFs, Ni/CNFs, PdNi/CNFs-1:2 and commercial RuO_2 catalyst for OER; **c** Polarization curves and **d** corresponding Tafel plots of the Pd/CNFs, Ni/CNFs, PdNi/CNFs-1:2 and commercial Pt/C catalyst for HER in 1 M KOH electrolyte; **e** EIS of the Pd/CNFs, Ni/CNFs and PdNi/CNFs-1:2 at the potential of 1.60 V versus RHE (the inset shows the equivalent circuit of the fitted curves); **f** chronoamperometric response (j-t) curve of PdNi/CNFs-1:2 at a constant potential of 1.60 V versus RHE (the inset shows a digital image of the O_2 bubbles formed on the PdNi/CNFs-1:2 membrane during the electrocatalytic process). Reprinted with permission from Ref. [85]. Copyright 2017, Elsevier Ltd

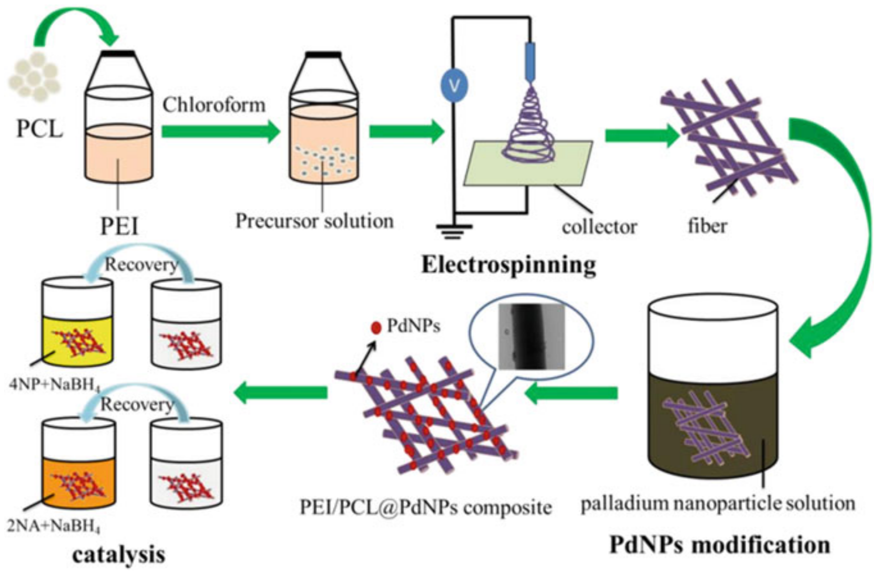

Fig. 17 Preparation process of polyethyleneimine/polycaprolactone/Pd nanoparticles (PEI/PCL@PdNPs) composite and its catalytic performances. Reprinted with permission from Ref. [97]. Copyright 2019, MDPI Ltd

surface area of electrospun fibers and provide an active site for the loading of palladium particles, so the added PEI component effectively adjusts the microscopic morphology of PEI/PCL fibers. The obtained PEI/PCL@PdNPs catalysts for the reduction of 4-nitrophenol (4-NP) and 2-nitroaniline (2-NA) showed very effective, stable, and reusable catalytic performance. It is worth mentioning that the reaction rate constant of 4-NP catalytic reduction is 0.16597 s^{-1}. Therefore, we have developed a highly efficient catalyst with potential application prospects in the field of catalysis and water treatment (Fig. 17 and 18).

The stability and recyclability of the catalyst are another aspect of evaluating the catalyst. Therefore, it is very important and necessary to explore the repetitive catalytic capabilities of PEI/PCL@PdNPs catalysts for 4-NP and 2-NA, as shown in Fig. 19. The catalytic efficiency of PEI/PCL@PdNPs catalysts after repeated catalytic reduction of fresh 4-NP and 2-NA systems for 8 cycles was 95% and 92%, respectively. The above results indicate that the PEI/PCL@PdNPs catalyst has high catalytic activity, stability, and recyclability. Referring to the previous literature, the catalytic efficiency has hardly decreased, which is attributed to the adhesion of organic matter on the catalyst surface and the loss of palladium particles on the catalyst surface during the washing of PEI/PCL@PdNPs with ethanol and ultrapure water [98]. This work provides new research clues for the preparation of composite materials loaded with PdNPs and ideal metal particle-based carriers.

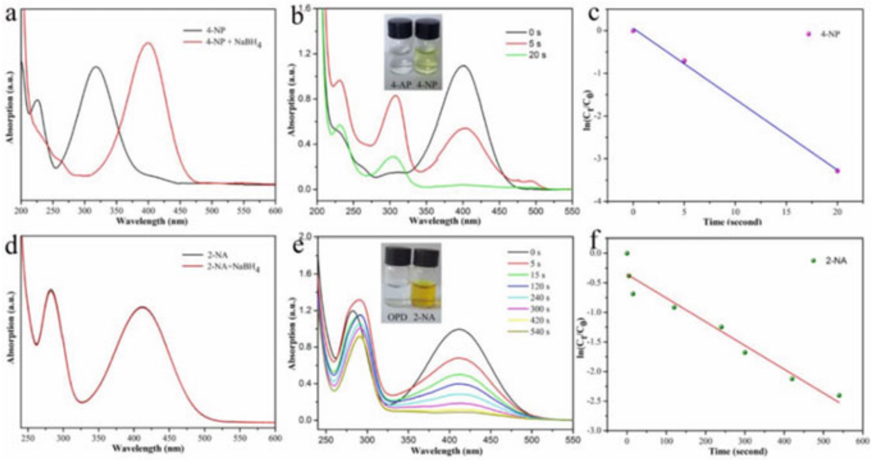

Fig. 18 UV absorption curves of 4-NP and 2-NA before and after adding NaBH4 aqueous solution (**a**, **d**); catalytic reduction of 4-NP and 2-NA with PEI/PCL@PdNPs composite (PEI:PCL, w/w, 35:65) and photographs of 4-NP and 2-NA solution after reduction (**b**, **e**); the linear relationship of the reduction process (**c**, **f**). Reprinted with permission from Ref. [97]. Copyright 2019, MDPI Ltd

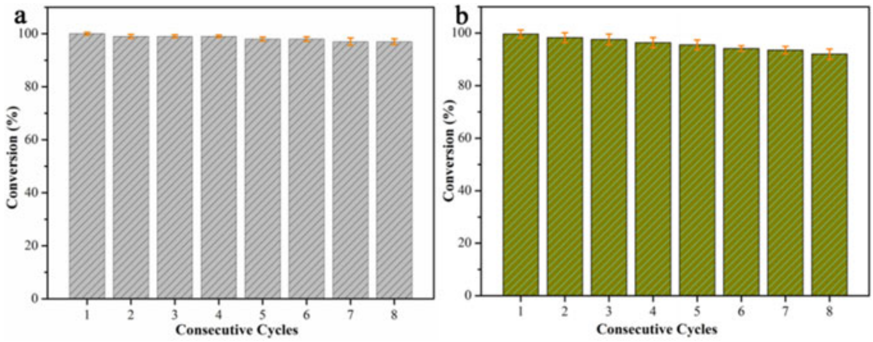

Fig. 19 Recyclability test of PEI/PCL@PdNPs catalyst for the reduction of 4-NP (**a**) and 2-NA (**b**). Reprinted with permission from Ref. [97]. Copyright 2019, MDPI Ltd

4 Hierarchical Electrospun Nanofibers Treated by Solvent Vapor Annealing as Air Filtration Mat for High-Efficiency PM2.5 Capture

In the past few years, environmental issues have received extensive attention due to their danger to human health and the environment [99–101]. Particulate matter (PM) is a very complex mixture of pollutants, with very fine particles and small droplets [102]. PM2.5 is particularly harmful because these small particles can penetrate the lungs and bronchi [30, 103–107]. In an indoor environment, these particles can be filtered through ventilation or central air-conditioning system, and the personal protection of outdoor personnel is not good, because most commercial masks have low PM2.5 removal efficiency because of their small diameter particles. Therefore, how to effectively and conveniently remove these PM pollutants from the air has become an urgent and challenging problem for researchers. For example, designing and developing high-efficiency filter materials that can efficiently remove PM2.5 particles are the central focus: evidence-based, high porosity, high accumulation of filter fibers. When the fiber diameter is small and the fiber diameter is large, the removal efficiency of PM2.5 is higher. As we all know, electrospinning is a relatively simple method for producing continuous fibers with nanometer and submicron diameters. The fibers prepared by electrospinning have high porosity, fine pore size, staggered pore structure, small pore size, and controllable diverse structure and thickness, which make them ideal for air filtration materials.

Huang et al. introduced a new type of high-efficiency air filter mat that can be used for outdoor protection [108]. The nanocomposite of the new high-efficiency air filter was successfully made of poly (ε-caprolactone)/polyethylene oxide (PCL/PEO) using electrospinning technology and solvent vapor annealing (SVA). The SVA treatment gives the fiber surface a wrinkle effect and enhances the PM2.5 capture ability of the protective mask. This nano-wrinkled air filter mat can effectively filter PM2.5 under severe pollution conditions (PM2.5 particle concentration is higher than 225 mg m^{-3}), and the removal efficiency is 80.01%. Field tests have shown that the air filter mat has a high PM2.5 removal efficiency under dense fog. Compared with commercial masks, the manufactured SVA-treated PCL/PEO air filter pads have a simpler, greener, and more environmentally friendly preparation process and have excellent degradation characteristics, with a wide range of potential applications and high filtration efficiency (Figs. 20, 21 and 22).

5 Conclusions and Remarks

In summary, as a simple and widely used technology, electrospinning can satisfy people's desire to quickly prepare nanofiber materials from a wide range of materials. By studying the composition, structure, porosity, surface, and fiber orientation of nanofibers, fiber properties can be selectively tailored for various applications. Although nanofibers have broad application prospects in heterogeneous catalysis and biomedical research, they still face a series of challenges, such as low dispersibility and uncontrollable degradability. With the precise control of the nanofiber microstructure, the preparation of surface-active nanofiber sponges will provide the possibility of developing flexible and recyclable catalytic systems. As a scaffold polymer nanofiber for tissue regeneration, its design, composition, and structure still need to be further optimized in clinical applications. Currently, the preparation of nanofibers is still in the laboratory research stage, the fiber output is low, mass production cannot be achieved, and industrialization is difficult to achieve. Although the electrospinning method is simple and can prepare a variety of nanofibers

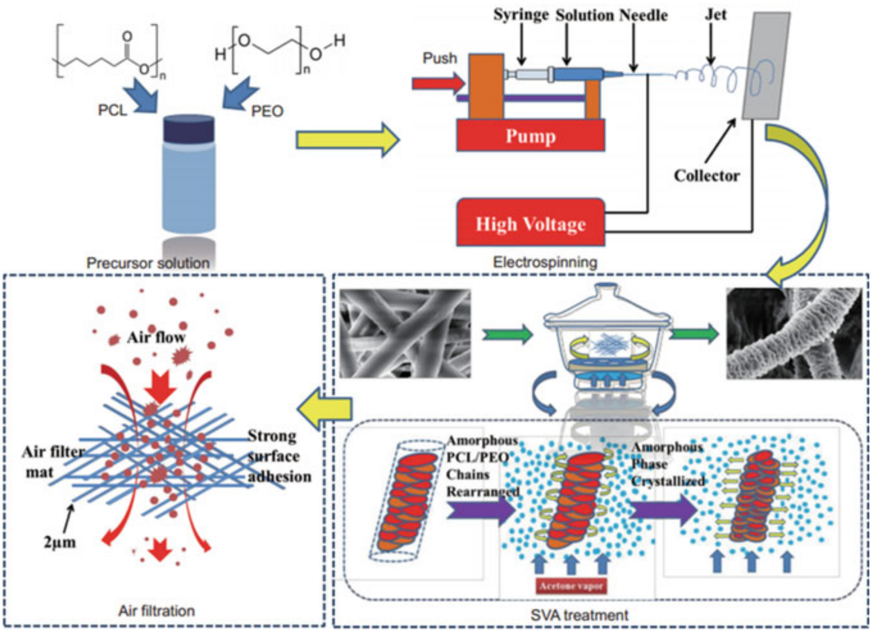

Fig. 20 A schematic illustration of the preparation and filtration of the obtained electrospun nanowrinkled air filtration mat. Reprinted with permission from Ref. [108]. Copyright 2019, Springer Ltd

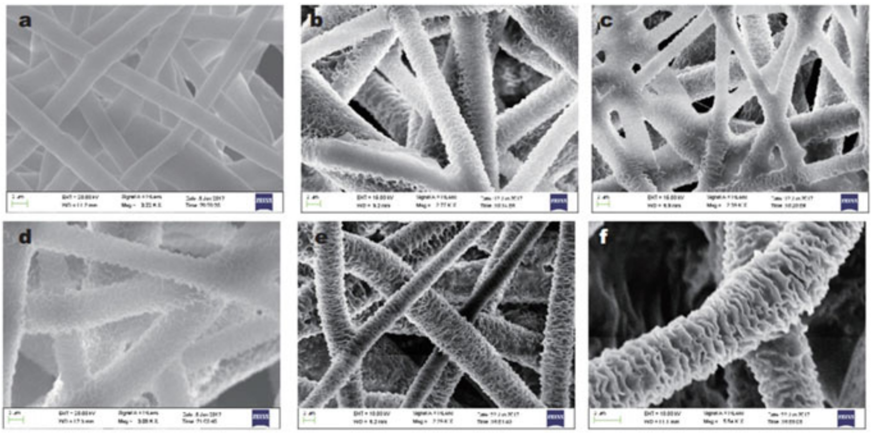

Fig. 21 SEM images of the prepared electrospun PCL/PEO nanofibers (**a**, Sample 1) and SVA treatment at different time intervals: **b** one day; **c** 2 days; **d** 3 days; **e** 4 days; **f** 5 days. Reprinted with permission from Ref. [108]. Copyright 2019, Springer Ltd

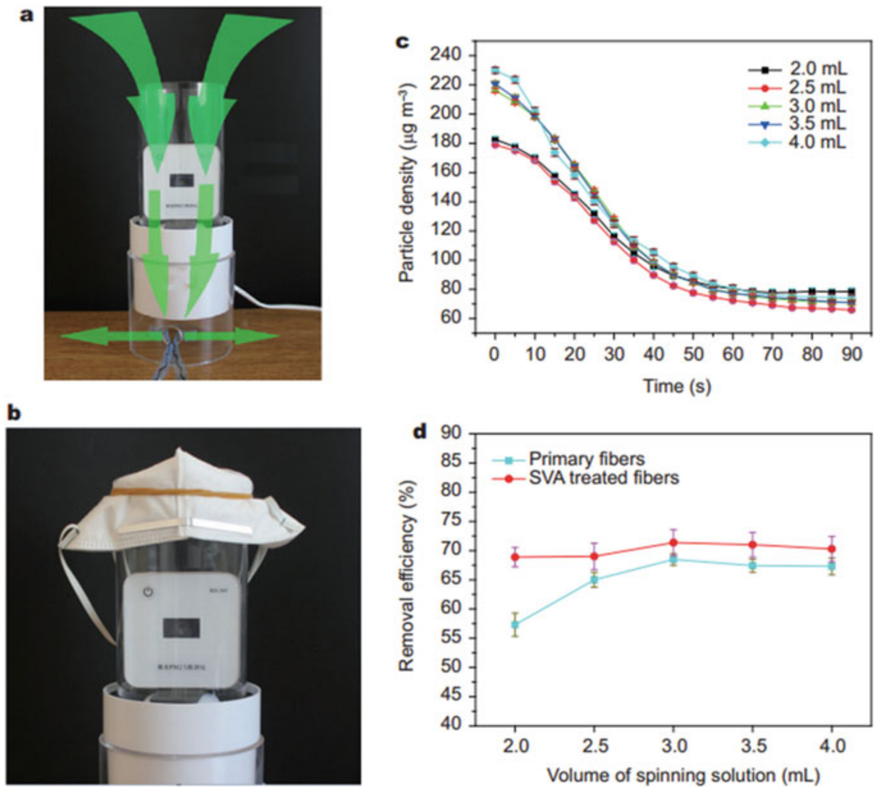

Fig. 22 Schematics of the air filtration mat that captured PM2.5 by airflow (**a**) and working state with mask filtration (**b**); **c** PM2.5 filtration curves for the air filtration mat (Sample 1) with different volumes of spinning precursor solution; **d** PM2.5 removal efficiency plots for primary fibers and SVA-treated fibers. Reprinted with permission from Ref. [108]. Copyright 2019, Springer Ltd

with different compositions, different structures, and different arrangements, there are still many challenges. For example, the nanofibers prepared by electrospinning cannot obtain filaments separated from each other, and the yield is low, and the strength Low, which limits the application. At present, people have made some breakthroughs in these problems. By simulating the complex spatial distribution of natural tissue, the three-dimensional scaffold has functional grading in terms of composition, arrangement, porosity, and pore size, which will make it better for tissue regeneration applications. It is believed that in the near future, electrospinning technology will be fully developed, and eventually from laboratory to industry, from basic research to clinical application.

Acknowledgements We greatly appreciate the financial supports of National Natural Science Foundation of China (No. 21872119), the Talent Engineering Training Funding Project of Hebei Province (No. A201905004), and the Research Program of the College Science and Technology of Hebei Province (No. ZD2018091).

References

1. Bhardwaj N, Kundu S (2010) Electrospinning: a fascinating fiber fabrication technique. Biotechnol Adv 28:325–347
2. Simons H (1966) Process and apparatus for producing patteined non woven fabrics .US3280229
3. Doshi J, Reneker D (1995) Electrospinning process and applications of electrospun fibers. J Electrostat 35:151–160
4. Ju J, Kang W, Li L (2016) Preparation of poly(tetrafluoroethylene) nanofiber film by electro-blown spinning method. Mater Lett 171:236–239
5. Yang D, Li EZ, Guo W (2011) Research and industrial development of nanofibers prepared by electrospinning. Mater Rev 25:64–68
6. Li M, Zhang J, Liu X, Wang Y (2016) Synthesis of high performance SAPO-34 zeolite membrane by a noveltwo-step hydrothermal synthesis dry gel conversion method. Micropor Mesopor Mat 225:261–271
7. Anton F (1975) Process and apparatus for preparing artificial threads: U.S. Patent 504:1934-10-2
8. Yan X, Gevelber M (2017) Electrospinning of nanofibers: characterization of jet dynamics and humidity effects. Part Sci Technol 35:139–149
9. Yao J, Bastiaansen C, Peijs T (2014) High strength and high modulus electrospun nanofibers. Fibers 2:158–186
10. Zhang X, Dai H, Cao Y (2013) Fabrication of high-strength aligned multi-walled carbon nanotubes/polyvinyl alcohol composite nanofibers by electrospinning. Adv Mater Res 796:311–316
11. Wang J, Zhang Z, Zhang Q, Liu J, Ma J (2018) Preparation and adsorption application of carbon nanofibers with large specific surface area. J Mater Sci 53:16466–16475
12. Wang W, Wang H, Wang H, Jin X, Li J, Zhu Z (2018) Electrospinning preparation of a large surface area, hierarchically porous, and interconnected carbon nanofibrous network using polysulfone as a sacrificial polymer for high performance supercapacitors. RSC Adv 8:28480–28486
13. Miao Y, Wang R, Chen D, Liu Z, Liu T (2012) Electrospun self-standing membrane of hierarchical SiO_2@γ-AlOOH (Boehmite) core/sheath fibers for water remediation. ACS Appl Mater Inter 4:5353–5359
14. Greiner A, Wendorff J (2007) Electrospinning: a fascinating method for the preparation of ultrathin fibers. Angew Chem Int Ed 46:5670–5703
15. Wang X, Yu J, Sun G, Ding B (2016) Electrospun nanofibrous materials: a versatile medium for effective oil/water separation. Mater Today 19:403–414
16. Wang Q, Liu S, Fu L, Cao Z, Ye W, Li H, Guo P, Zhao XS (2018) Electrospun γ-Fe_2O_3 nanofibers as bioelectrochemical sensors for simultaneous determination of small biomolecules. Anal Chim Acta 1026:125–132
17. Xue Z, Huang L, Wang C (2016) Sonocrystallization of ZIF-8 on electrostatic spinning TiO_2 nanofibers surface with enhanced Photocatalysis property through synergistic effect. ACS Appl Mater Inter 8:20274
18. Fan L, Xue M, Kang Z, Li H, Qiu S (2012) Electrospinning technology applied in zeolitic imidazolate framework membrane synthesis. J Mater Chem 22:25272–25276
19. Lu W, Sun J, Jiang X (2014) Recent advances in electrospinning technology and biomedical applications of electrospun fibers. J Mater Chem B 2:2369–2380
20. Choi S, Persano L, Camposeo A, Jang J, Koo W, Kim S, Cho H, Kim I, Pisignano D (2017) Electrospun nanostructures for high performance chemiresistive and optical sensors. Macromol Mater Eng 302:1600569
21. Bai Y, Liu Y, Li Y (2017) Mille-feuille shaped hard carbons derived from polyvinylpyrrolidone via environmentally friendly electrostatic spinning for sodium ion battery anodes. Rsc Adv 7:5519–5527

22. Hu X, Liu S, Zhou G, Huang Y, Xie Z, Jing X (2014) Electrospinning of polymeric nanofibers for drug delivery applications. J Control Release 185:12–21
23. Liu J, Bauer A, Li B (2014) Solvent vapor annealing: An efficient approach for inscribing secondary nanostructures onto electrospun fibers. Macromol Rapid Commun 35:1503–1508
24. Lu Q, Yu Y, Ma Q, Chen B, Zhang H (2016) 2D Transition-metal-dichalcogenide-nanosheet-based composites for photocatalytic and electrocatalytic hydrogen evolution reactions. Adv Mater 28:1917–1933
25. Lin J, Ding B, Yang J, Yu J, Sun G (2012) Subtle regulation of the micro-and nanostructures of electrospun polystyrene fibers and their application in oil absorption. Nanoscale 4:176–182
26. Si Y, Wang X, Li Y, Chen K, Wang J, Yu J, Wang H, Ding B (2014) Optimized colorimetric sensor strip for mercury (II) assay using hierarchical nanostructured conjugated polymers. J Mater Chem A 2:645–652
27. Liu Y, Hou C, Jiao T, Song J, Zhang X, Xing R, Zhou J, Zhang L, Peng Q (2018) Self-assembled AgNP-containing nanocomposites constructed by electrospinning as efficient Dye photocatalyst materials for wastewater treatment. Nanomaterials 8:35. https://doi.org/10.3390/nano8010035
28. Panaitescu D, Ionita E, Nicolae C, Gabor A, Dinescu G (2018) Poly(3-hydroxybutyrate) modified by nanocellulose and plasma treatment for packaging applications. Polymers 10:1249
29. Rauwel P, Rauwel E, Uhl W (2019) Application and behavior of nanomaterials in water treatment. Nanomaterials
30. Xing R, Wang W, Jiao T, Ma K, Zhang Q, Hong W, Qiu H, Zhou J, Zhang L, Peng Q (2017) Bioinspired polydopamine sheathed nanofibers containing carboxylate graphene oxide nanosheet for high-efficient dyes scavenger. ACS Sustain Chem Eng 5:4948–4956
31. Qiu H, Liang C, Yu J, Zhang Q, Song M, Chen F (2017) Preferable phosphate sequestration by nano-La(III) (hydr)oxides modified wheat straw with excellent properties in regeneration. Chem Eng J 315:345–354
32. Zhang Q, Teng J, Zou G, Peng Q, Du Q, Jiao T, Xiang J (2016) Efficient phosphate sequestration for water purification by unique sandwich-like MXene/magnetic iron oxide nanocomposites. Nanoscale 8:7085–7093
33. Bao Q, Zhang H, Yang J, Wang S, Tang D, Jose R, Ramakrishna S, Lim C, Loh K (2010) Graphene-polymer nanofiber membrane for ultrafast photonics. Adv Funct Mater 20:782–791
34. Hou C, Jiao T, Xing R, Chen Y, Zhou J, Zhang L (2017) Preparation of TiO_2 nanoparticles modified electrospun nanocomposite membranes toward efficient dye degradation for wastewater treatment. J Taiwan Inst Chem E 78:118–126
35. Luan V, Tien H, Hur S (2015) Fabrication of 3D structured ZnO nanorod/reduced graphene oxide hydrogels and their use for photo-enhanced organic dye removal. J Colloid Inter Sci 437:181–186
36. Zhou W, Ding C, Jia X, Tian Y, Guan Q, Wen G (2015) Self-assembly of Fe_2O_3/reduced graphene oxide hydrogel for high Li-storage. Mater Res Bull 62:19–23
37. Sun Y, Cheng Y, He K, Zhou A, Duan H (2015) One-step synthesis of three-dimensional porous ionic liquid-carbon nanotube-graphene gel and MnO_2-graphene gel as freestanding electrodes for asymmetric supercapacitors. RSC Adv 5:10178–10186
38. Jiao T, Zhao H, Zhou J, Zhang Q, Luo X, Hu J, Peng Q, Yan X (2015) Self-assembly reduced graphene oxide nanosheet hydrogel fabrication by anchorage of chitosan/silver and its potential efficient application toward dyes degradation for wastewater treatments. ACS Sustain Chem Eng 3:3130–3139
39. Huang H, Ren P, Chen J, Zhang W, Ji X, Li Z (2012) High barrier graphene oxide nanosheets/poly(vinyl alcohol) nanocomposite films. J Membrane Sci 409–410:156–163
40. Balandin A, Ghosg S, Bao W, Calizo I (2008) Superior thermal conductivity of single-layer graphene. Nano Lett 8:902–907
41. Lee H, Dellatore S, Miller W, Messersmith P (2007) Mussel-inspired surface chemistry for multifunctional coatings. Science 318:426–430

42. Waite J, Qin X (2001) Polyphosphoprotein from the adhesive pads of mytilus edulis. Biochemistry 40:2887–2893
43. Ryu J, Lee Y, Kong W, Kim T, Park T, Lee H (2011) Catechol-functionalized chitosan/pluronic hydrogels for tissue adhesives and hemostatic materials. Biomacromol 12:2653–2659
44. Phua S, Yang L, Toh C, Huang S, Tsakadze Z, Lau S, Mai Y, Lu X (2012) Reinforcement of polyether polyurethane with dopamine-modified clay: the role of interfacial hydrogen bonding. ACS Appl Mater Inter 4:4571–4578
45. Yang H, Lan Y, Zhu W, Li W, Xu D, Cui J, Shen D, Li G (2012) Polydopamine-coated nanofibrous mats as a versatile platform for producing porous functional membranes. J Mater Chem 22:994–17001
46. Son H, Ryu J, Lee H, Nam Y (2013) Silver-polydopamine hybrid coatings of electrospun poly(vinyl alcohol) nanofibers. Macromol Mater Eng 298:547–554
47. Gao H, Sun Y, Zhou J, Xu R, Duan H (2013) Mussel-inspired synthesis of polydopamine-functionalized graphene hydrogel as reusable adsorbents for water purification. ACS Appl Mater Interfaces 5:425–432
48. Zhang S, Zhang Y, Bi G, Liu J, Wang Z, Xu Q, Lui H, Li X (2014) Mussel-inspired polydopamine biopolymer decorated with magnetic nanoparticles for multiple pollutants removal. J Hazard Mater 270:27–34
49. Yu Y, Shapter J, Popelka-Filcoff R, Bennett J, Ellis A (2017) Copper removal using bio-inspired polydopamine coated natural zeolites. J Hazard Mater 273:174–182
50. Yan J, Huang Y, Miao Y, Tjiu W, Liu T (2015) Polydopamine-coated electrospun poly(vinyl alcohol)/poly(acrylic acid) membranes as efficient dye adsorbent with good recyclability. J Hazard Mater 283:730–739
51. Li L, Guo X, Fu L, Prudhomme R, Lincoln S (2008) Complexation behavior of α-, β-, and γ-cyclodextrin in modulating and constructing polymer networks. Langmuir 24:8290–8296
52. Guo X, Wang J, Li L, Chen Q, Li Z, Pham D, May B, Prud'homme R, Easton C (2010) Tunable polymeric hydrogels assembled by competitive complexation between cyclodextrin dimers and adamantly substituted poly(acrylate)s. AIChE J 56:3021–3024
53. Wang J, Pham D, Guo X, Li L, Pham D, Luo Z, Ke H, Zheng L, Prud'homme R (2009) Polymeric networks assembled by adamantyl and β-cyclodextrin substituted poly(acrylate)s: host-guest interactions, and the effects of ionic strength and extent of substitution. Ind Eng Chem Res 49:609–612
54. Theron J, Walker J, Cloete T (2008) Nanotechnology and water Treatment: applications and emerging opportunities. Criti Rev Microbiol 34:43–69
55. Leudjo T, Pillay K, Yangkou M (2017) Nanosponge cyclodextrin polyurethanes and their modification with nanomaterials for the removal of pollutants from waste water: a review. Carbohyd Polym 159:94–107
56. Khaoulani S, Chaker H, Cadet C, Bychkov E, Cherifaouali L, Bengueddach A, FourmentinS (2015) Wastewater treatment by cyclodextrin polymers and noble metal/mesoporous TiO_2 photocatalysts. C R Chim18: 23–31
57. Yamasaki H, Makihata Y, Fukunaga K (2010) Efficient phenol removal of wastewater from phenolic resin plants using crosslinked cyclodextrin particles. J Chem Technol Biotechnol 81:1271–1276
58. Chai K, Ji H (2012) Dual functional adsorption of benzoic acid from wastewater by biological-based chitosan grafted β-cyclodextrin. Chem Eng J 203:309–318
59. Li J, Loh X (2008) Cyclodextrin-based supramolecular architectures: syntheses, structures, and applications for drug and gene delivery. Adv Drug Deliv Rev 60:1000–1017
60. Yilmaz E, Memon S, Yilmaz M (2010) Removal of direct azo dyes and aromatic amines from aqueous solutions using two β-cyclodextrin-based polymers. J Hazard Mater 174:592–597
61. Cui H, Bai M, Lin L (2018) Plasma-treated poly(ethylene oxide) nanofibers containing tea tree oil/beta-cyclodextrin inclusion complex for antibacterial packaging. Carbohyd Polym 179:360–369
62. Celebioglu A, Uyar T (2017) Antioxidant Vitamin E/cyclodextrin inclusion complex electrospun nanofibers: enhanced water solubility, prolonged shelf life, and photostability of Vitamin E. J Agric Food Chem 65:5404–5412

63. Guo R, Wang R, Yin J, Jiao T, Huang H, Zhao X, Zhang L, Li Q, Zhou J, Peng Q (2019) Fabrication and highly efficient dye removal characterization of beta-cyclodextrin-based composite polymer fibers by electrospinning. Nanomaterials 9:127
64. Lin L, Dai Y, Cui H (2017) Antibacterial poly(ethylene oxide) electrospun nanofibers containing cinnamon essential oil/beta-cyclodextrin proteoliposomes. Carbohyd Polym 178:131–140
65. Narayan R, Kim J, Kim J, Lee K, Kim S (2016) Graphene oxide liquid crystals: discovery, evolution and applications. Adv Mater 28:3045–3068
66. Zeng J, Hou H, Wendorff J, Greiner A (2004) Electrospun poly(vinyl alcohol)/poly(acrylic acid) fibres with excellent water-stability. E-Polymers 4:899–906
67. Wang X, Lu X, Liu B, Chen D, Tong Y, Shen G (2014) Flexible energy storage devices design consideration and recent progress. Adv Mater 26:4763–4782
68. Yin J, Zhan F, Jiao T, Deng H, Zou G, Bai Z, Zhang Q, Peng Q (2020) Highly efficient catalytic performances of nitro compounds via hierarchical PdNPs-loaded MXene/polymer nanocomposites synthesized through electrospinning strategy for wastewater treatment. Chinese Chem Lett. https://doi.org/10.1016/j.cclet.2019.08.047
69. Li L, Peng S, Wu H, Yu L, Madhavi S, Lou X (2015) A Flexible quasi-solid-state asymmetric Electrochemical capacitor Based on hierarchical porous V_2O_5 nanosheets on carbon nanofibers. Adv Energy Mater 5:1500753
70. Li Y, Dai H (2014) Recent advances in zinc-air batteries. Chem Soc Rev 43:5257
71. Nam G, Park J, Choi M, Oh P, Park S, Kim M, Park N, Cho J, Lee J (2015) Single crystalline pyrochlore nanoparticles with metallic conduction as efficient bi-functional oxygen electrocatalysts for Zn-air batteries. ACS Nano 9:6493
72. Jin Y, Chen F (2018) Bifunctional electrocatalysts for Zn–air batteries. Electrochim Acta 2:39–67
73. Liu Q, Wang Y, Dai L, Yao J (2016) Scalable fabrication of nanoporous carbon fiber films as bifunctional catalytic electrodes for flexible zn-air batteries. Adv. Mater. 28:3000–3006
74. Strmcnik D, Lopes P, Genorio B, Stamenkovic V, Markovic N (2016) Design principles for hydrogen evolution reaction catalyst materials. Nano Energy 29:29–36
75. Tahir M, Mahmood N, Zhang X, Mahmood T, Butt F, Aslam I, Tanveer M, Idrees F, Khalid S, Shakir I, Yan Y, Zou J, Cao C, Hou Y (2015) Bifunctional catalysts of Co_3O_4@GCN tubular nanostructured (TNS) hybrids for oxygen and hydrogen evolution reactions. Nano Res. 8:3725–3736
76. Safizadeh F, Ghali E, Houlachi G (2015) Electrocatalysis developments for hydrogen evolution reaction in alkaline solutions. Int J Hydrogen Energy 40:256–274
77. Popczun E, Mckone J, Read C, Biacchi A, Wiltrout A, Lewis N, Schaak R (2013) Nanostructured nickel phosphide as an electrocatalyst for the hydrogen evolution reaction. J Am Chem Soc 135:9267
78. Kanan M, Nocera D (2008) In situ formation of an oxygen-evolving catalyst in neutral water containing phosphate and Co^{2+}. Science 321:1072–1075
79. Mcintyre N, Cook M (1975) X-ray photoelectron studies on some oxides and hydroxides of cobalt, nickel, and copper. Anal Chem 47:2208–2213
80. Bergmann A, Zaharieva I, Dau H, Strasser P (2013) Electrochemical water splitting by layered and 3D cross-linked manganese oxides: correlating structural motifs and catalytic activity. Energ Environ Sci 6:2745–2755
81. Khan S, Khan S, Asiri A (2016) Electro-catalyst based on cerium doped cobalt oxide for oxygen evolution reaction in electrochemical water splitting. J Mater Sci Mater E 27:1–9
82. Lee Y, Suntivich J, May K, Perry E, Shao-Horn Y (2012) Synthesis and activities of rutile IrO2 and RuO2 nanoparticles for oxygen evolution in acid and alkaline solutions. J Phys Chem Lett 3:399–404
83. Kibsgaard J, Jaramillo T (2015) Molybdenum phosphosulfide: an active, acidStable, earth-abundant catalyst for the hydrogen evolution reaction. Angew Chem Int Ed 53:14433–14437
84. Nong H, Oh H, Reier T, Willinger E, Willinger M, Petkov V, Teschner D, Strasser P (2015) Oxide-supported IrNiO(x) core-shell particles as efficient, costeffective, and stable catalysts for electrochemical water splitting. Angew Chem Int Ed Eng 54:2975–2981

85. Chen J, Chen D, Yu D, Zhang M, Zhu H, Du M (2017) Carbon nanofiber-supported PdNi alloy nanoparticles as highly efficient bifunctional catalysts for hydrogen and oxygen evolution reactions. Electrochim Acta 246:17–26
86. Lukatskaya M, Mashtalir O, Ren C, Dall'Agnese Y, Rozier P, Taberna P, Naguib M, Simon P, Barsoum M, Gogotsi Y (2013) Cation intercalation and high volumetric capacitance of two-dimensional titanium carbide. Science 341:1502–1505
87. Jian M, Wang C, Wang Q, Wang H, Xia K, Yin Z, Zhang M, Liang X, Zhang Y (2017) Advanced carbon materials for flexible and wearable sensors. Sci China Mater 60:1206–1062
88. Li Z, Wang L, Sun D, Zhang Y, Liu B, Hu Q, Zhou A (2015) Synthesis and thermal stability of two-dimensional carbide MXene Ti_3C_2. Mater Sci Eng B 191:33–40
89. Naguib M, Mochalin V, Barsoum M, Gogotsi Y (2013) 25th anniversary article: MXenes: a new family of two-dimensional materials. Adv Mater 26:992–1005
90. Li J, Du Y, Huo C, Wang S, Cui C (2015) Thermal stability of two-dimensional Ti_2C nanosheets. Ceram Int 41:2631–2635
91. Miranda A, Halim J, Barsoum M, Lorke A (2016) Electronic properties of freestanding $Ti_3C_2T_x$ MXene monolayers. Appl Phys Lett 108:033102
92. Boota M, Anasori B, Voigt C, Zhao M, Barsoum M, Gogotsi Y (2015) Pseudocapacitive electrodes produced by oxidant-free polymerization of pyrrole between the layers of 2D titanium carbide (MXene). Adv Mater 28:1517–1522
93. Wang H, Zhang J, Wu Y, Huang H, Li G, Zhang X, Wang Z (2016) Surface modified MXene Ti_3C_2, multilayers by aryl diazonium salts leading to large-scale delamination. Appl Surf Sci 384:287–293
94. Karlsson L, Birch J, Halim J, Barsoum M, Persson P (2015) Atomically resolved structural and chemical investigation of single MXene sheets. Nano Lett 15:4955–4960
95. Huang X, Wang R, Jiao T, Zou G, Zhan F, Yin J, Zhang L, Zhou J, Peng Q (2019) Facile preparation of hierarchical AgNP-loaded MXene/Fe_3O_4/polymer nanocomposites by electrospinning with enhanced catalytic performance for wastewater treatment. ACS Omega 4:1897–1906
96. Amezquita-Garcia H, Razo-Flores E, Cervantes F, Rangel-Mendez J (2013) Activated carbon fibers as redox mediators for the increased reduction of nitroaromatics. Carbon 55:276–284
97. Wang C, Yin J, Han S, Jiao T, Bai Z, Zhou J, Zhang L, Peng Q (2019) Preparation of palladium nanoparticles decorated polyethyleneimine/polycaprolactone composite fibers constructed by electrospinning with highly efficient and recyclable catalytic performances. Catalysts 9:559
98. Guo R, Jiao T, Xing R, Chen Y, Guo W, Zhou J, Zhang L, Peng Q (2017) Hierarchical AuNPs-loaded Fe_3O_4/polymers nanocomposites constructed by electrospinning with enhanced and magnetically recyclable catalytic capacities. Nanomaterials 7:317
99. Zhang R, Jing J, Tao J, Hsu S, Wang G, Cao J, Lee C, Zhu L, Chen Z, Zhao Y (2013) Chemical characterization and source apportionment of PM2.5 in Beijing: seasonal perspective. Atmos Chem Phys 13:7053–7074
100. Li K, Jiao T, Xing R, Zou G, Zhou J, Zhang L, Peng Q (2018) Fabrication of tunable hierarchical MXene@AuNPs nanocomposites constructed by self-reduction reactions with enhanced catalytic performances. Sci China Mater 61:728–736
101. Cheng C (2005) Interfacial behaviors of PMMA-PEO block copolymers at the air/water interface. Sci China Ser B 48:567–573
102. Zhao H, Jiao T, Zhang L, Zhou J, Zhang Q, Peng Q, Yan X (2015) Preparation and adsorption capacity evaluation of graphene oxide-chitosan composite hydrogels. Sci China Mater 58:811–818
103. Sun Z, Liao T, Kou L (2017) Strategies for designing metal oxide nanostructures. Sci China Mater 60:1–24
104. Wang R, Liu Q, Jiao T, Li J, Rao Y, Su J, Bai Z, Peng Q (2019) Facile preparation and enhanced catalytic properties of self-assembled Pd nanoparticle-loaded nanocomposites films synthesized via electrospun approach. ACS Omega 4:8480–8486
105. Zhou J, Liu Y, Jiao T, Xing R, Yang Z, Fan J, Liu J, Li B, Peng Q (2018) Preparation and enhanced structural integrity of electrospun poly(ε-caprolactone)-based fibers by freezing amorphous chains through thiol-ene click reaction. Colloids Surface A 538:7–13

106. Wang C, Yin J, Wang R, Jiao T, Huang H, Zhou J, Zhang L, Peng Q (2019) Facile preparation of self-assembled polydopamine-modified electrospun fibers for highly effective removal of organic dyes. Nanomaterials 9:116
107. Wang C, Sun S, Zhang L, Yin J, Jiao T, Zhang L, Xu Y, Zhou J, Peng Q (2019) Facile preparation and catalytic performance characterization of AuNPs-loaded hierarchical electrospun composite fibers by solvent vapor annealing treatment. Colloids Surface A 561:283–291
108. Huang X, Jiao T, Liu Q, Zhang L, Zhou J, Li B, Peng Q (2019) Hierarchical electrospun nanofibers treated by solvent vapor annealing as air filtration mat for high-efficiency PM2.5 capture. Sci China Mater 62:423–436